

Thiadiazolopyrimidines as Acid Corrosion Inhibitors for Mild Steel

S.Chitra[†], K.Parameswari, M.Vidhya, M.Kalishwari, and A.Selvaraj¹

Dept. of Chemistry, P.S.G.R. Krishnammal College for Women, Coimbatore

¹Dept. of Chemistry, CBM College, Coimbatore

(Received October 25, 2010; Revised February 23, 2011; Accepted February 25, 2011)

The inhibitive action of thiadiazolopyrimidines on mild steel in 1 M H₂SO₄ has been studied using weight loss, gasometric studies and electrochemical polarization and AC impedance measurements. The effect of temperature on the corrosion behaviour of mild steel in 1 M H₂SO₄ with optimum concentration of inhibitors was studied in the temperature ranging from 313-333K. The adsorption of the inhibitor on the surface of mild steel was found to be exothermic, spontaneous and followed the mechanism of physisorption. The adsorption of these compounds on mild steel surface was found to obey Langmuir adsorption isotherm. The protective film formed on the surface of mild steel by the adsorption of inhibitor in 1 M H₂SO₄ solution was confirmed by optical microscopic technique. Synergistic effect of halide ions on mild steel in 1 M H₂SO₄ was studied by weight loss technique.

Keywords : corrosion, inhibitor, thiadiazolopyrimidines, mild steel

1. Introduction

The corrosion of steel is a fundamental academic and industrial concern that has received a considerable amount of attention.¹⁾ Acid solutions are widely used in industry. Some of the important fields of application being acid pickling of iron and steel, chemical cleaning and processing, ore production and oil well acidification. The heavy loss of metals as a result of its contact with acids can be minimized by the use of inhibitors.²⁾ Inorganic compounds like chromates, phosphates, molybdates etc., and a variety of organic compounds containing hetero atoms like N, S and O are being investigated as corrosion inhibitors.³⁾⁻⁶⁾ Among them, nitrogen containing heterocyclic compounds are considered to be effective corrosion inhibitors on steel in acid media.⁷⁾ N-heterocyclic compound inhibitors act by adsorption on the metal surface and the adsorption takes place through nitrogen hetero atom as well as the triple or conjugated double bonds or aromatic rings in their molecular structures.

2. Experimental method

Mild steel strips containing C, 0.084%, P, 0.025%, Mn, 0.369%, S, 0.027% and the remaining iron were used for the measurement of weight loss and gasometric studies.

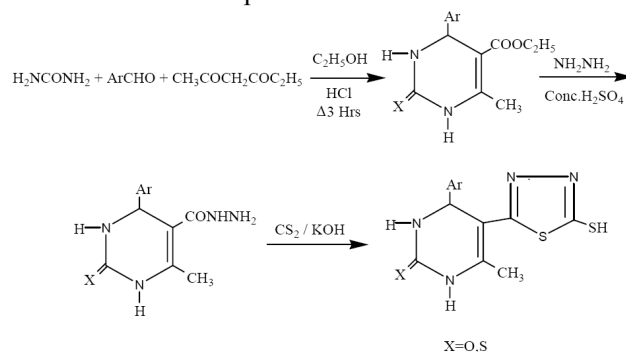
For electrochemical studies, a cylindrical mild steel rod of the same composition embedded in Teflon with an exposed area of 0.785 cm² was used. All the chemicals used for the synthesis of the inhibitors are of analar grade.

2.1 Synthesis of inhibitors

Thiadiazolopyrimidines (PTDA 1-6) were synthesized by the procedure reported by Pandhy et al.⁸⁾

Synthesis was carried out in three steps. In the first step carboethoxy pyrimidine-2-one/thione were prepared by the condensation of urea/thiourea, ethylacetoacetate and aromatic aldehyde in ethanol in the presence of catalytic amount of con. HCl. The esters were then converted into the corresponding hydrazides by reaction with hydrazine hydrate. The hydrazides were cyclised to thiadiazoles by reaction with KOH/CS₂.

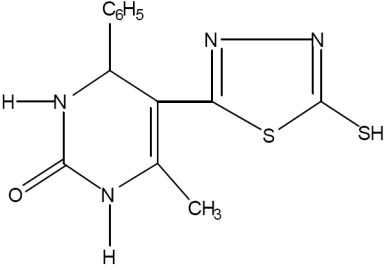
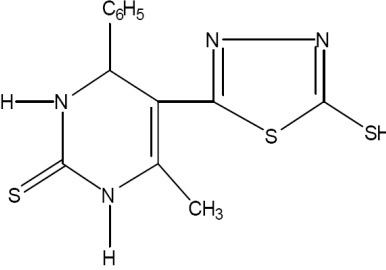
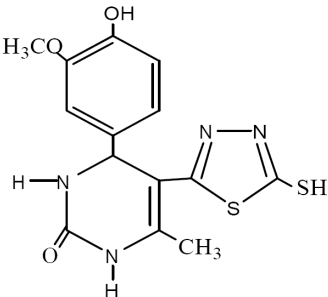
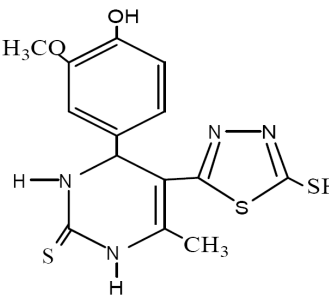
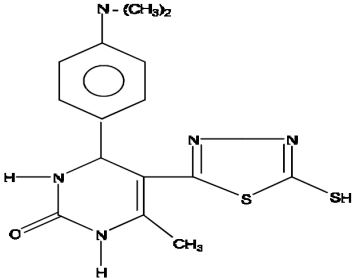
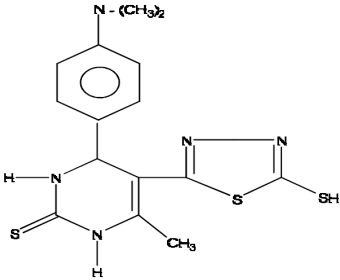
The reactions are presented in scheme 1.



Scheme 1

[†] Corresponding author: rajshree1995@rediffmail.com

Table 1. Structure of the synthesised inhibitors

 <p>4-(phenyl)-5-(5'-mercaptothiadiazolo)-6-methylpyrimidine-2-one PTDA 1</p>	 <p>4-(phenyl)-5-(5'-mercaptothiadiazolo)-6-methylpyrimidine-2-thione PTDA 2</p>
 <p>4-(3'-methoxy, 4'-hydroxyphenyl)-5-(5'-mercaptothiadiazolo)-6-methyl pyrimidine-2-one PTDA 3</p>	 <p>4-(3'-methoxy, 4'-hydroxyphenyl)-5-(5'-mercaptothiadiazolo)-6-methyl pyrimidine-2-thione PTDA 4</p>
 <p>4-(4'-N, N-dimethylaminophenyl)-5-(5'-mercaptothiadiazolo)-6-methyl-2-pyrimidine-2-one PTDA 5</p>	 <p>4-(4'-N, N-dimethylaminophenyl)-5-(5'-mercaptothiadiazolo)-6-methyl-2-pyrimidine-2-thione PTDA 6</p>

Structures of synthesized inhibitors are presented in Table 1.

The synthesised inhibitors were characterized by IR spectra. The IR spectra of PTDA 6 is given in Fig. 1

2.2 Non-electrochemical methods

2.2.1 Weight loss (coupon) method

Mild steel specimens of size 5 cm × 2 cm × 0.05 cm were used for weight loss method. The mild steel specimens were polished with emery papers of 1/0 to 4/0 grades and degreased with trichloroethylene. The specimens were suspended into the experimental solution (200 ml) containing 1 M H₂SO₄ and different concentrations of the inhibitors. The initial weights of the specimens were noted.

After three hours, the specimens were removed, washed with running water, dried and weighed. From the initial and final masses of the specimens, the loss in mass was calculated. Inhibition efficiency (IE) and corrosion rate were calculated using the following equations.

Efficiency of inhibitor =

$$\frac{(\text{Weight loss without inhibitor} - \text{Weight loss with inhibitor})}{\text{Weight loss without inhibitor}} \times 100$$

Corrosion Rate (mpy) =

$$\frac{534 \times \text{Weight loss in mgms}}{\text{Density} \times \text{area in sq.inch} \times \text{Time in hrs}}$$

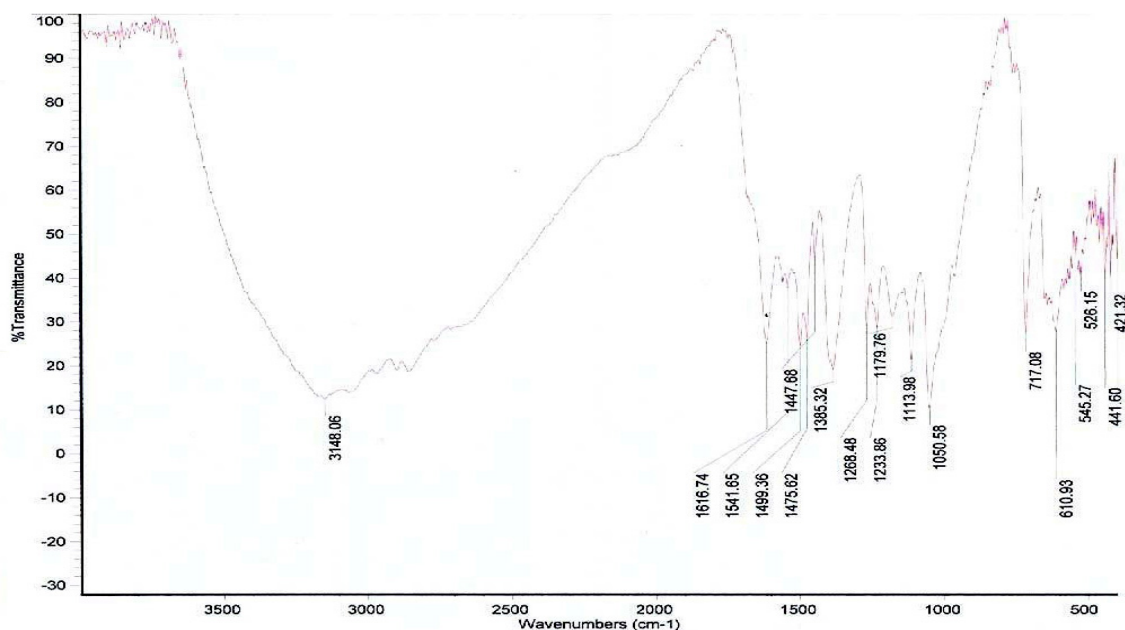


Fig. 1. IR SPECTRA OF PTDA 6.

The weight loss method was repeated at higher temperatures from 313-333K at a concentration of 2.5 mM of the inhibitors.

2.3 Gasometric method

The efficiency of the inhibitors was also determined by gasometric technique from the volume of H_2 gas collected in the absence and presence of inhibitors at $30 \pm 1^\circ C$. The inhibition efficiency was calculated using the formula,

$$\text{Inhibition efficiency}(\%) = \frac{V_B - V_I}{V_B} \times 100$$

where V_B & V_I are volume of H_2 evolved in the absence and presence of inhibitors.

2.4 Electrochemical techniques

Electrochemical measurements were carried out using the potentiostat Solartron, U.K. model 1208 B.

2.4.1 Potentiodynamic polarisation studies

Polarisation studies were carried out in a conventional three electrode glass cell assembly with a platinum counter electrode and saturated calomel electrode (SCE) as reference from a potential range of -200 mV to +200 mV with respect to open circuit potential at a scan rate of 1 mV/sec for mild steel, both in the presence and absence of inhibitors. Polarisation measurement were performed to evaluate the corrosion kinetic parameters such as I_{Corr} , E_{Corr} and Tafel slopes b_a and b_c .

$$\text{Inhibition efficiency}(\%) = \frac{I_{corr}(\text{blank}) - I_{corr}(\text{inh})}{I_{corr}(\text{blank})} \times 100$$

where I_{corr} and $I_{corr}(\text{inh})$ are the corrosion current in the absence and presence of inhibitors.

2.4.2 Electrochemical impedance measurements

The electrochemical impedance measurements were carried out at corrosion potential over a frequency range of 10 KHz to 0.01 Hz with single amplitude of 10 mV for mild steel in acidic media. Impedance measurements were carried out for mild steel in 1 M H_2SO_4 with and without inhibitors for the selected concentrations of the inhibitors. Inhibitor efficiency was calculated using the formula,

$$\text{Inhibition efficiency}(\%) = \frac{R_t(\text{inh}) - R_t(\text{blank})}{R_t(\text{inh})} \times 100$$

where $R_t(\text{inh})$ & $R_t(\text{blank})$ are charge transfer resistance obtained in the absence and presence of the inhibitors.

2.5 Synergistic effect

The synergistic inhibitions of mild steel in 1 M H_2SO_4 by a combination of PTDA and halide ions have been studied using weight loss method. The mild steel specimens were immersed in 1 M H_2SO_4 containing various concentrations of the inhibitor and 1 mM halide ions each for a duration of 3hrs. From the weight loss, the inhibition efficiency and corrosion rate were calculated.

Table 2. Inhibition efficiencies of various concentrations of the inhibitors for corrosion of mild steel in 1 M H₂SO₄ obtained by weight loss measurement at 30±1°C

Name of the inhibitor	Concentration (mM)	Weight loss (g)	Inhibition efficiency (%)	Degree of surface coverage (Θ)	Corrosion rate (mpy)
PTDA1	Blank	0.5056	-	-	-
	0.1	0.2564	49.29	0.4929	1945.05
	0.15	0.2129	57.89	0.5789	1615.05
	0.25	0.1881	62.79	0.6279	1426.9
	0.5	0.1131	77.63	0.7763	857.9
	1	0.0399	92.11	0.9211	302.76
	1.5	0.0313	93.81	0.9381	237.5
	2.5	0.0248	95.09	0.9509	188.21
PTDA2	Blank	0.5056	-	-	-
	0.1	0.2238	55.74	0.5574	1697.75
	0.15	0.1455	71.22	0.7122	1103.76
	0.25	0.0505	90.01	0.9001	383.47
	0.5	0.0236	95.13	0.9513	179.41
	1	0.0092	98.18	0.9818	69.79
	1.5	0.0107	97.88	0.9788	81.17
	2.5	0.0067	98.67	0.9867	51.36
PTDA3	Blank	0.5056	-	-	-
	0.1	0.3613	28.54	0.2854	2740.8
	0.15	0.3522	30.34	0.3034	2671.78
	0.25	0.3317	34.39	0.3439	2516.27
	0.5	0.2947	41.71	0.4171	2235.59
	1	0.2365	53.22	0.5322	1794.09
	1.5	0.2285	54.81	0.5481	1733.4
	2.5	0.2142	57.63	0.5763	1624.9
PTDA4	Blank	0.5056	-	-	-
	0.1	0.4066	19.58	0.1958	3084.47
	0.15	0.3852	23.81	0.2381	2922.13
	0.25	0.3328	34.18	0.3418	2524.6
	0.5	0.3156	37.57	0.3757	2394.14
	1	0.2635	47.88	0.4788	1998.91
	1.5	0.2325	54.01	0.5401	1763.75
	2.5	0.1829	63.82	0.6382	1387.5
PTDA5	Blank	0.5056	-	-	-
	0.1	0.0970	80.81	0.8081	735.84
	0.15	0.0606	88.01	0.8801	459.71
	0.25	0.0293	94.20	0.9420	222.27
	0.5	0.0195	96.14	0.9614	147.9
	1	0.0155	96.93	0.9693	117.58
	1.5	0.0110	97.82	0.9782	83.45
	2.5	0.0079	98.43	0.9843	59.93
PTDA6	Blank	0.5056	-	-	-
	0.1	0.0854	83.11	0.8311	647.9
	0.15	0.0262	94.81	0.9481	198.8
	0.25	0.0184	96.36	0.9636	139.7
	0.5	0.0118	97.67	0.9767	89.60
	1	0.0069	98.63	0.9863	52.34
	1.5	0.0053	99.05	0.9905	40.21
	2.5	0.0009	99.82	0.9982	7.05

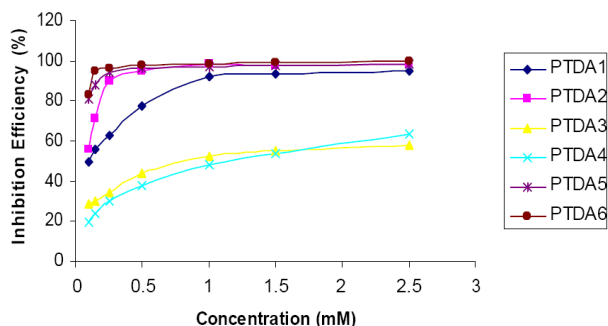


Fig. 2. Plot of Inhibition efficiency (%) Vs concentration (mM) for the inhibition of corrosion of mild steel in 1 M H₂SO₄.

3. Results and discussion

3.1 Weight loss studies

Table 2 shows the values of inhibition efficiency (IE) and corrosion rate (CR) obtained from weight loss measurements at different concentrations of inhibitors at 30 °C. It has been found that the weight loss decreases and inhibition efficiency of the thiadiazolopyrimidine derivatives (PTDA 1-6) increases with increase in inhibitor concentration (Fig. 2). The maximum inhibition efficiency was achieved at 2.5 mM concentration for all the inhibitors (except PTDA 3 and PTDA 4). The efficiency of the compounds is due to the presence of π -electrons of aromatic rings and lone pair of electrons on nitrogen and sulphur atoms. Schmitt⁹⁾ reported that a mixture of nitrogen and sulphur containing compounds are better inhibitors than either type alone. The decrease in corrosion rate with increase in inhibitor concentration is due to increase in surface coverage Θ , which shows that the compounds form a protective adsorptive layer on the surface. Thus adsorption forms the mechanism of inhibition.

3.2 Effect of temperature

The results obtained for the corrosion of mild steel in 1 M H₂SO₄ in the absence and presence of PTDA 1-6 in the temperature range 30-60 °C (Table 3) revealed that increase in temperature increases corrosion rate and decreases the inhibition efficiency at 2.5 mM concentration of the inhibitors. According to Dehri and Ozcan¹⁰⁾ the relationship between temperature dependence of inhibition efficiency (%) of an inhibitor and the activation energy (E_a) found in its presence is as follows (a) Inhibitors whose inhibition efficiency (%) decrease with temperature increase, the value of activation energy (E_a) found is greater than that in the uninhibited solution. (b) Inhibitors whose inhibition efficiency (%) does not change with temperature variation, the activation energy (E_a) does not change with

the presence or absence of inhibitors. (c) Inhibitors whose inhibition efficiency (%) increases with temperature increase, the value of activation energy (E_a) is less than that in the inhibited solution.

In an acidic solution the corrosion rate is related to temperature by the Arrhenius equation,

$$\log CR = \frac{-E_a}{2,303 RT} + \log A \quad (1)$$

where 'CR' is the corrosion rate, ' E_a ' is the apparent activation energy, 'R' is the molar gas constant, 'T' is the absolute

Table 3. Inhibition efficiencies of 2.5 mM concentration of various inhibitors for corrosion of mild steel in 1 M H₂SO₄ obtained by weight loss measurement at higher temperature

Name of the inhibitor	Temperature (K)	Weight loss (g)	Inhibition efficiency (%)	Corrosion rate (mpy)
Blank	303	0.5056	-	-
	313	0.3029	-	-
	323	0.4865	-	-
	333	0.8084	-	-
PTDA1	303	0.0248	95.09	188.13
	313	0.0239	92.11	543.89
	323	0.0410	91.57	933.04
	333	0.0684	91.53	1556.58
PTDA2	303	0.0067	98.67	50.82
	313	0.0049	98.38	111.51
	323	0.0104	97.86	236.67
	333	0.0213	97.37	484.72
PTDA3	303	0.2142	57.63	1624.9
	313	0.1426	52.92	3245.15
	323	0.2813	42.18	6401.54
	333	0.5504	31.91	12525.45
PTDA4	303	0.1829	63.83	1387.48
	313	0.1200	60.38	2730.84
	323	0.1957	59.77	4453.54
	333	0.329	59.30	7487.05
PTDA5	303	0.0079	98.44	59.93
	313	0.005	98.35	113.79
	323	0.009	98.15	204.81
	333	0.0202	97.50	459.69
PTDA6	303	0.0009	99.82	6.827
	313	0.0015	99.50	34.14
	323	0.0031	99.36	70.55
	333	0.0052	99.35	118.34

temperature and 'A' is the frequency factor.

The values of E_a were computed from the slope of the Arrhenius plots (Fig. 3) and are listed in Table 4. It is clear from the Table 4 that E_a values in the presence of additives are higher than that in the absence. The higher activation energies imply a slow reaction and that the reaction is very sensitive to temperature. The increase in E_a signifies physical adsorption. This conclusion is denoted by the decrease in inhibition efficiency with increasing temperature.

The standard free energy of adsorption ΔG_{ads}^0 was calculated using the relation

$$k = \frac{1}{55.5} \exp \left[\frac{\Delta G_{ads}^0}{RT} \right] \quad (2)$$

where 55.5 is the concentration of water in solution in moles/litre. The negative values of ΔG_{ads}^0 (Table 4) ensure the spontaneity of the adsorption process and the stability of the adsorbed layer. Generally values of ΔG_{ads}^0 upto -20 KJmol^{-1} are consistent with physisorption, while those around -40 KJ mol^{-1} or higher is associated with chemisorption as a result of sharing or transfer of electrons from organic molecules to metal surface.¹¹⁾ Enthalpy and Entropy of activation ΔH^0 and ΔS^0 were obtained by applying the transition state equation. Plots of $\log (CR/T)$ as a function of $1/T$ were made (Fig. 4). Straight lines were obtained with slope $(-\Delta H^0/R)$ and an intercept $(\ln R/N_h + \Delta S^0/R)$ from which the values of ΔH^0 and ΔS^0 were calculated and listed in Table 5. While an endothermic adsorption process ($\Delta H^0 > 0$) is attributed unequivocally to chemisorptions, an exothermic adsorption process ($\Delta H^0 < 0$) may involve either physisorption or chemisorption or a mixture of both processes. In the present work, the negative value obtained may introduce both chemisorption and physisorption processes. This may be interpreted by the presence of hetero atoms nitrogen, oxygen/sulphur which leads to co-ordinate bonds, and aromatic rings which get physisorbed. Also the negative values of ΔH^0 show that the adsorption is exothermal with an ordered phenomenon

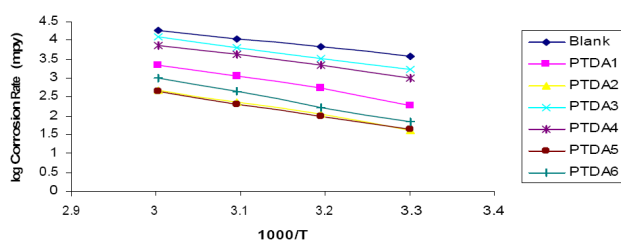


Fig. 3. Arrhenius plots for mild steel in 1 M H_2SO_4 solution in the absence and presence of inhibitors.

Table 4. Activation energies (E_a) and free energy of adsorption (ΔG_{ads}^0) for the corrosion of mild steel in 1 M H_2SO_4 at 2.5 mM concentration of the inhibitors

Name of the inhibitor	E_a (kJ)	ΔG_{ads}^0 at various temperatures (kJ)			
		303 K	313 K	323 K	333 K
Blank	43.63	-	-	-	-
PTDA1	68.34	-6.63	-6.28	-6.39	-6.58
PTDA2	76.24	-10.30	-9.49	-9.50	-9.77
PTDA3	55.43	-3.03	-3.64	-3.25	-2.82
PTDA4	68.03	-8.10	-8.14	-8.14	-8.07
PTDA5	63.91	-7.93	-8.12	-8.25	-8.13
PTDA6	56.94	-4.01	-3.98	-4.08	-4.18

Table 5. Kinetic/Thermodynamic Parameters for mild steel corrosion in 1 M H_2SO_4

Name of the Inhibitor	E_a KJ/mole	$-\Delta H^0$ KJ/mole	$-\Delta S^0$ KJ/mole
Blank	0.0408	0.0177	0.130
PTDA1	0.0641	0.0278	0.106
PTDA2	0.0637	0.0277	0.116
PTDA3	0.0526	0.0229	0.116
PTDA4	0.0507	0.0220	0.120
PTDA5	0.0511	0.0222	0.126
PTDA6	0.0631	0.0274	0.104

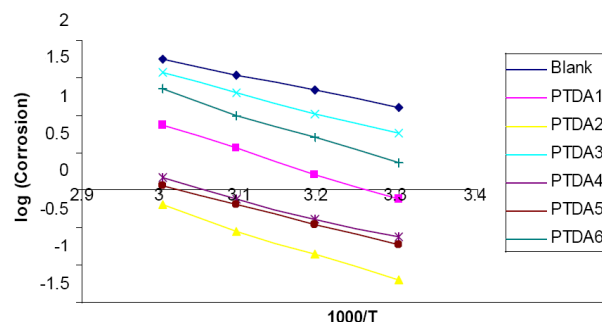


Fig. 4. Transition state plot for mild steel corrosion in 1 M H_2SO_4 in the absence and presence of 2.5 mM concentration of the inhibitor.

ascribed by the negative values of ΔS^0 .¹²⁾ The negative value of ΔS^0 decreases in the presence of inhibitor as compared to that in their absence i.e., there is an increase in randomness or disorder on the surface due to the adsorption process and also desorption at higher temperatures.

3.3 Adsorption isotherm

It is generally accepted that organic molecules inhibit corrosion by adsorption at the metal/solution interface and that the adsorption depends on the chemical composition of the molecule, the temperature and the electrochemical potential at the metal/ solution interface. The solvent water molecules could also adsorb at metal/solution interface.¹³⁾ Hence the adsorption of organic inhibitor molecules from the aqueous solution can be regarded as a quasi substitution process between the organic compound in the aqueous phase ($Org_{(sol)}$) and water molecules at the electrode surface ($H_2O_{(ads)}$).¹⁴⁾



where 'x' is the size ratio, (ie.,) the number of water molecules replaced by one molecule of organic inhibitor. Basic information of the adsorption of inhibitor on metal surface can be provided by an adsorption isotherm. Attempts were made to fit experimental data to various isotherms including Frumkin, Langmuir, Temkin, Freundlich, Bockris-Swinkels and Flory-Huggins isotherms. The Langmuir isotherm was found to fit well with the experimental data. The adsorption isotherm of Langmuir is represented by the following equation,

$$K = \frac{\theta}{C(1-\theta)} \quad (4)$$

Rearranging this equation,

$$\frac{C}{\theta} = \frac{1}{K} + C \quad (5)$$

where ' θ ' is the degree of surface coverage, 'K' is the equilibrium constant of the adsorption process and 'C' is the inhibitor concentration. It was found that a plot of C/θ Vs C is a straight line for all the inhibitors. Fig. 5 depicts the graph of the Langmuir adsorption isotherm for the compounds. As adsorption is of Langmuir character it can be concluded that the organic molecules are attached as a monolayer and through a physical mechanism.

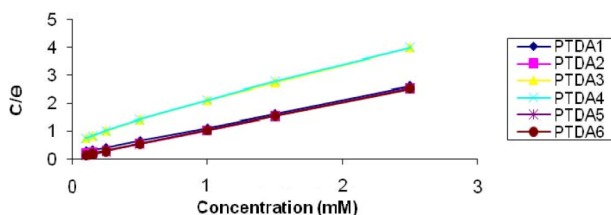


Fig. 5. Langmuir plot of inhibitors in 1 M H₂SO₄.

Table 6. Inhibition efficiencies for the selected concentrations of the inhibitors for the corrosion of mild steel in 1 M H₂SO₄ obtained by gasometric measurement

Name of the inhibitor	Concentration (mM)	Volume of gas (cc)	Inhibition efficiency (%)
	Blank	26.4	-
PTDA1	0.1	13.6	48.48
	0.25	9.5	64.02
	1	2.37	91.02
	2.5	0.88	96.67
PTDA2	0.1	11.97	54.66
	0.25	2.45	90.73
	1	0.44	98.35
	2.5	0.29	98.89
PTDA3	0.1	19.11	27.61
	0.25	17.05	35.40
	1	12.64	52.12
	2.5	10.83	58.99
PTDA4	0.1	21.02	20.38
	0.25	16.19	38.69
	1	13.32	49.55
	2.5	9.25	64.98
PTDA5	0.1	4.89	81.44
	0.25	1.74	93.42
	1	1.06	95.98
	2.5	0.39	98.52
PTDA6	0.1	4.16	84.21
	0.25	1.21	95.43
	1	0.50	98.11
	2.5	0.084	99.68

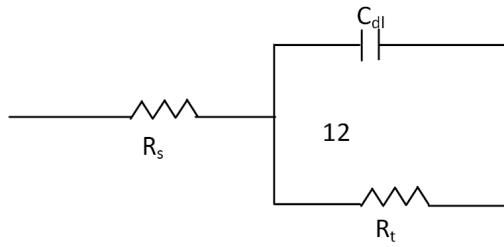
3.4 Gasometric studies

Table 6 gives the values of inhibition efficiency obtained using gasometric method from the volume of gas collected in the absence and presence of inhibitors at constant temperature of about $30 \pm 1^\circ\text{C}$ for the corrosion of mild steel in 1 M H₂SO₄. The volume of gas collected decreased with increase in the concentration of the inhibitor. There is a good agreement between the values of inhibition efficiency obtained from weight loss method and gasometric measurements.

3.5 Electrochemical studies

3.5.1 Electrochemical behaviour of impedance

A simple electrode reaction such as metal deposition or metal dissolution can be represented by a modified equivalent circuit



R_s - series resistance
 R_t - charge transfer resistance
 C_{dl} - double layer capacitance

By adopting complex plane analysis for the total cell impedance Z , Sluyters et al.,¹⁵⁾ have resolved it into real and imaginary components as,

$$Z' = R_s + \frac{R_t + \sigma\omega^{-1/2}}{(\sigma\omega^{-1/2} C_{dl} + 1)^2 + \omega^2 C_{dl}^2 (R_t + \sigma\omega^{-1/2})^2} \quad (6)$$

$$Z'' = \frac{WC_{dl}(R_t + \sigma\omega^{-1/2})^2 + \sigma^2 C_{dl} + \sigma\omega^{-1/2}}{(\sigma\omega^{-1/2} C_{dl} + 1)^2 + \omega^2 C_{dl}^2 (R_t + \sigma\omega^{-1/2})^2} \quad (7)$$

The simplified equation for cell impedance is

$$Z' - \left[R_s - \frac{R_t^2}{2} \right] + [Z''] = \frac{R_t^2}{4} \quad (8)$$

which is the equation of a semi circle (Z'' vs. Z' -constant concentration) with its centre on Z' axis at $Z' = R_s T_{1/2} R_t$ and radius $1/2 R_t$. The interactions with the Z' axis are at $Z' = R_s$ for $\omega = a$ and at $Z' = R_s + R_t$ for $\omega = 0$. These are called Nyquist plots. With an increase in inhibitor concentration, the radius of the semicircle increases, the double layer capacitance C_{dl} decreases. In the current investigation also for all the tested inhibitors C_{dl} decreases with increase in inhibitor concentration (Table 7, Fig. 6) obviously due to increased adsorption as required by theory. These observations have been supported by the findings of Selvaraj^{16,17)} in the study of effect of adsorption of ethylamine on the reduction of Pd (II) on the dropping mercury electrode.

3.5.2 Polarization behaviour of inhibition

Analysis of the polarization data in Table 8 reveals that E_{corr} values are only slightly shifted in the presence of the inhibitors, I_{corr} values decrease with increase in the concentration of the inhibitors. The Tafel constants b_a and b_c are both affected but b_c is affected to a greater extent (Fig. 7). Hence it can be concluded that although all the inhibitors behave as mixed type but more cathodic in nature.

Table 7. AC-impedance parameters for corrosion of mild steel for selected concentrations of the inhibitors in 1 M H₂SO₄

Name of the inhibitor	Concentration (mM)	R_t (ohm cm ²)	$2C_{dl}$ (μF/cm ²)	Inhibition efficiency (%)
Blank	0	10.5299	34.2381	-
PTDA1	0.1	60.54	9.0297	82.62
	0.5	80.23	6.9159	86.89
	2.5	117.46	5.5556	91.04
PTDA2	0.1	65.74	11.56	83.98
	0.5	118.03	6.933	91.08
	2.5	359.72	5.8049	97.07
PTDA3	0.1	22.94	11.397	54.10
	0.5	26.89	9.6651	60.84
	2.5	62.54	7.7213	83.16
PTDA4	0.1	63.55	7.4837	83.43
	0.5	69.11	7.1954	84.76
	2.5	78.64	6.2964	86.61
PTDA5	0.1	81.07	8.3109	87.01
	0.5	83.27	7.8445	87.37
	2.5	186.44	7.6712	94.35
PTDA6	0.1	277.82	3.8764	96.21
	0.5	751.01	2.6752	98.60
	2.5	802.34	1.9733	98.69

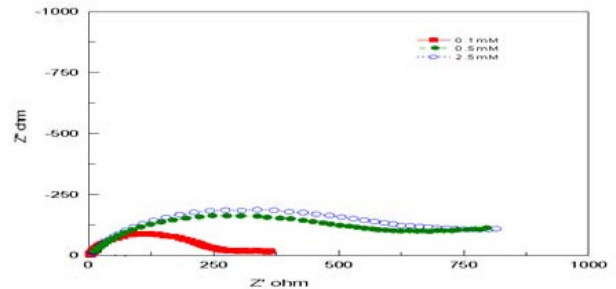


Fig. 6. Nyquist diagram for mild steel in 1 M H₂SO₄ for selected concentrations of inhibitor PTDA 6.

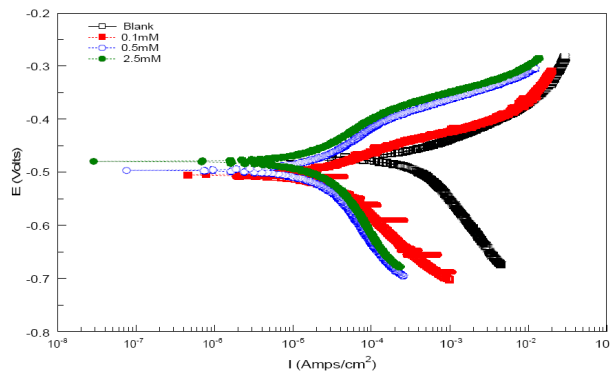


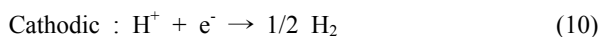
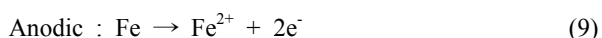
Fig. 7. Polarization curves for mild steel in 1 M H₂SO₄ for selected concentrations of inhibitor PTDA 6.

Table 8. Corrosion parameters for corrosion of mild steel with selected concentrations of the inhibitors in 1 M H₂SO₄ by potentiodynamic polarization method

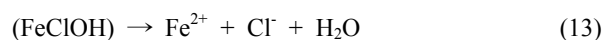
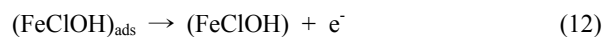
Name of the inhibitor	Concentration	Tafel slopes (mV/dec)		E _{corr} (mV)	I _{corr} (μAmp/cm ²)	Inhibition efficiency (%)
		b _a	B _c			
Blank	0	150.034	158.506	-0.4540	1725.0	-
PTDA1	0.1	153.99	334.82	-0.4879	231.16	86.60
	0.5	172.54	389.12	-0.4917	217.11	87.41
	2.5	142.22	299.09	-0.5119	145.89	91.54
PTDA2	0.1	135.89	263.81	-0.5420	109.18	93.67
	0.5	60.135	115.04	-0.5384	21.147	98.77
	2.5	54.412	87.452	-0.4952	20.614	98.80
PTDA3	0.1	131.48	275.27	-0.5290	875.64	49.24
	0.5	117.35	248.39	-0.5428	628.00	63.59
	2.5	120.52	281.06	-0.5150	539.00	68.75
PTDA4	0.1	128.65	298.38	-0.5247	689.52	60.05
	0.5	113.3	228.04	-0.5331	610.78	64.59
	2.5	88.542	176.15	-0.5496	242.82	85.92
PTDA5	0.1	115.06	207.12	-0.5381	677.54	60.72
	0.5	75.177	132.02	-0.5379	123.62	92.83
	2.5	67.996	142.48	-0.5359	88.173	94.89
PTDA6	0.1	62.38	132.23	-0.5060	25.219	98.53
	0.5	83.515	168.50	-0.4970	17.503	98.99
	2.5	84.673	171.93	-0.4799	15.815	99.08

3.6 Synergistic effect

The synergistic influence of the added halide ions on the inhibition of mild steel corrosion by thiadiazolopyrimidine derivatives can be explained on the basis of a concept proposing the direct participation of halide ions in the mechanism of corrosion. According to this concept, corrosion of steel in acidic solution is the sum of the following reactions.



However each of these reactions proceeds through many consecutive steps depending on pH and type of anions present in the solution. There are two main theories for inhibition based on the work of Heusler¹⁸⁾ and Bockris.¹⁹⁾ Both theories indicate the participation of anions of the solutions directly. Anodic dissolution of iron in acidic medium can be written as



Adsorption of halide ions on the metal surface affects the above kinetics of dissolution of steel.

The inhibition efficiency values for the inhibitors in the presence of three halide ions are presented in Table 9. It indicates that the enhancement of efficiency follows the order $\text{I}^- > \text{Br}^- > \text{Cl}^-$. Such an observation has also been reported by early workers who found that the adsorption and inhibiting action of organic cations and halide ions on metals of iron group increases in sequence from Cl^- to Br^- and becomes maximum for I^- ions.

The gradation in synergism observed in the current work is due to the difference in the anion adsorption which is found to be the highest for I^- ions, little lesser for Br^- and least for Cl^- . In the adsorption process, the radii and electronegativity of the halides seem to have played a significant role. I^- ions with largest deformable electron shells and with least electronegativity ought to have formed strongest chemical bonds with the metal surface and hence exhibit highest degree of synergism compared to other halides.²⁰⁾

Table 9. Synergistic effect of 1 mM KCl / KBr / KI on the inhibition efficiency of inhibitors by weight loss method at 30±1°C

Name of the inhibitor	Concentration (mM)	Inhibition efficiency (%)			
		Without KCl, KBr and KI	With 1mM KCl	With 1mM KBr	With 1mM KI
PTDA1	0.1	49.29	61.45	69.32	88.67
	0.25	62.79	64.97	71.98	89.90
	1	92.11	94.13	96.19	98.15
PTDA2	0.1	83.11	84.40	87.98	94.98
	0.25	96.36	96.48	96.67	98.95
	1	98.63	98.97	99.01	99.37
PTDA3	0.1	15.79	25.36	39.40	50.29
	0.25	23.59	29.84	41.58	53.34
	1	30.35	45.62	50.99	55.76
PTDA4	0.1	20.56	39.48	41.28	73.58
	0.25	37.57	53.20	66.30	80.28
	1	47.88	62.30	78.66	85.39
PTDA5	0.1	80.81	81.03	87.74	90.30
	0.25	94.20	95.52	97.75	98.37
	1	96.93	97.70	98.32	99.01
PTDA6	0.1	55.74	69.39	74.70	98.36
	0.25	90.01	92.32	92.99	99.01
	1	98.18	98.54	98.84	99.89

3.7 Visual examination

The mild steel plates immersed for 3 hours in 1 M H₂SO₄ and in 1 M H₂SO₄ containing 2.5 mM PTDA1-6 were air dried and examined using an optical microscope (OLYMPUS BX51M). The photographed mild steel plates are shown in the Fig. 8. Much information about the surface morphology cannot be obtained from the photographs. Visual examination of the photographs reveals that the addition of the inhibitors results in the formation of a protective layer on the mild surface and protects it from corrosion.

3.8 Mechanism of inhibition

It is generally assumed that the adsorption of the inhibitors at the metal/aggressive solution interface is the first step in the inhibition mechanism.²¹⁾ Considering the dependence of inhibition efficiency on the concentration as represented in Fig. 2, it can be concluded that the inhibitor acts by adsorbing and blocking the available active centres for steel dissolution. The adsorption process is made possible due to the presence of hetero atoms such as N, O and S which are regarded as active adsorption

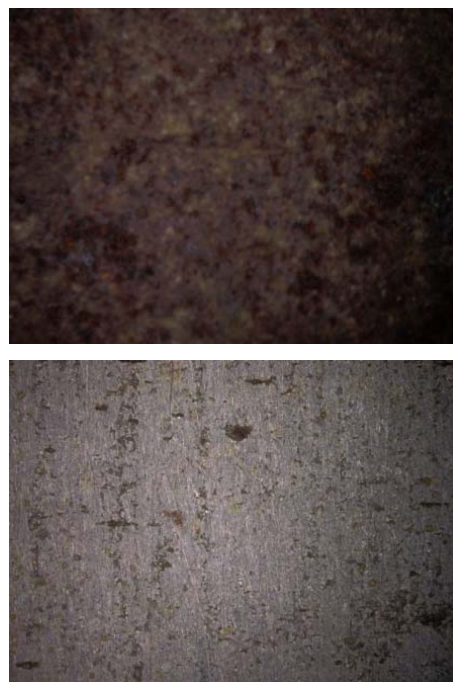


Fig. 8. Optical Microscope images of mild steel surface without and with the addition of PTDA 6.

centres. The thiadiazolopyrimidines PTDA 1,3,5 contain four nitrogen, two sulphur and one oxygen atoms and PTDA 2,4,6 contain four nitrogen and three sulphur atoms. Besides these compounds, contain a phenyl ring and two >C=N groups. The compounds could be adsorbed by the interaction between the lone pair of electrons of the oxygen, nitrogen and sulphur atoms, the electron rich π systems of the aromatic rings and the >C=N groups on the mild steel surface. This process as earlier reported by Umoren and Ebenso²²⁾ may be facilitated by the presence of vacant d-orbital of iron. The thiadiazolopyrimidines inhibit the corrosion by controlling both the anodic and cathodic reactions. In acidic solutions these compounds exist as protonated species. These protonated species adsorb on the cathodic sites of the mild steel and decreases the evolution of hydrogen. The positively charged protonated species facilitates adsorption of the compound on the metal surface through electrostatic interactions between the organic molecules and the metal surface.²³⁾

3.9 Evaluation of inhibitors

The order of inhibition efficiency of thiadiazolopyrimidin-2-one is

PTDA5> PTDA1>PTDA3

and thiadiazolopyrimidine-2-thione is

PTDA6> PTDA2>PTDA4

From the analysis of the inhibition efficiency data presented in Table 2, it is evident that due to the presence

of electron donating group $-NMe_2$ in the benzene rings. PTDA 5 & PTDA 6 display a maximum inhibition efficiency of 98.43 and 99.82 respectively. This may be due to the presence of 2- CH_3 groups (+I effect) which enhances the electron density on the nitrogen and thereby provide additional anchoring sites for adsorption. PTDA5 & PTDA6 have higher inhibition efficiency (IE) compared to the parent compounds PTDA1 & PTDA2 respectively. Similarly the inhibitors PTDA3 & PTDA4 are also expected to exhibit a higher inhibition efficiency due to the presence of electron donating $-OCH_3$ & $-OH$ group. But their inhibition efficiency values are less compared to the parent compounds PTDA1 & PTDA2. This decrease in inhibition efficiency may be attributed to the greater solubility of the hydroxy compound in aqueous acid medium leading to the dissolution of the inhibitor film from the metal surface. This is supported by the findings of Quraishi et al.²⁴ In general pyrimidine-2-thiones PTDA 2,4 & 6 have slightly higher inhibition efficiency compared to pyrimidine-2-ones PTDA 1,3 & 5. This may be due to presence of an additional sulphur atom in the pyrimidine-thiones.

4. Conclusions

The conclusions arrived based on the investigations are

1) The order of inhibition efficiency of the synthesized compounds at 2.5 mM concentration is

PTDA 5 > PTDA 1 > PTDA 3

PTDA 6 > PTDA 2 > PTDA 4

2) All the synthesised compounds are effective inhibitors for corrosion of mild steel in 1 M H_2SO_4 .

3) The inhibition efficiency increases with increase in inhibitor concentration and decreases with increasing temperature.

4) They inhibit corrosion by getting adsorbed on the metal surface following Langmuir adsorption isotherm.

5) The Tafel slopes obtained from potentiodynamic polarization curves indicate that all the inhibitors behave as mixed type but cathodic effect is more pronounced.

6) Addition of halide ions to the inhibitors shows an increase in inhibition efficiency. The synergistic influence of halide ion follows the order $I^- > Br^- > Cl^-$.

7) The inhibitive performance of pyrimidin-2-thiones is higher compared to pyrimidin-2-one.

References

1. F. Bentiss, M. Traisnel, and M. Lagrenee, *Corros. Sci.*, **42**, 127 (2000).
2. G. Trabaneli, *Corrosion*, **47**, 410 (1991).
3. S. A. M. Refacy, *Appl. Surf. Sci.*, **240**, 396 (2005).
4. M. A. Quraishi and H. K. Sharma, *J. Appl. Electrochem*, **35**, 33 (2005).
5. A. Ashassi-Sorkhavi, B. Shaaban, and D. Seifzadeh, *Appl. Surf. Sci.*, **239**, 239 (2005).
6. M. Bouklah, A. Ouassini, B. Hammouti, and A. E. Idrissi, *Appl. Surf. Sci.*, **252**, 2178 (2006).
7. F. Bentiss, M. Traisnel, L. Gengembre, and M. Lagrenee, *Appl. Surf. Sci.*, **161**, 194 (2000).
8. A. K. Pandhy, M. Bardhan, and S. Panda, *Indian J. Chem.*, **42B**, 910 (2003).
9. G. Schmitt, *British Corros. J.*, **19**, 99 (1984).
10. I. Dehri and M. Ozcan, *Mater. Chem. Phys.*, **98**, 316 (2006).
11. F. M. Donahue and K. Nobe, *J. Electrochem. Soc.*, **112**, 886 (1965).
12. E. E. Ebenso, H. Alemu, S. A. Umoren, and I. B. Obot, *Int. J. Electrochem. Sci.*, **3**, 1325 (2008).
13. J. Y. Zou and B. H. Yang, *Mater. Prot.*, **21**, 4 (1988).
14. M. Sahin, S. Bilgic, and H. Yilmaz, *Appl. Surf. Sci.*, **195**, 1 (2002).
15. J. H. Sluyters, *RECUEIL*, **79**, 1092 (1960).
16. A. Selvaraj and R. S. Subrahmanya, *J. Electrochem. Soc.*, **32**, 193 (1988).
17. A. Selvaraj and R. S. Subrahmanya, *J. Electrochem. Soc.*, **32**, 225 (1987).
18. K. E. Heusler, *J. Electrochem. Soc.*, **62**, 529 (1958).
19. J. O. M. Bockris, B. Drazic, and A. R. Drazic, *Electrochem. Acta*, **4**, 325 (1961).
20. Z. A. Iofa, V. V. Batrokov, and Cho NgokBa, *Zaschita Metallor*, **1**, 56 (1995).
21. L. Niu, H. Zhang, F. Wei, S. Wa, X. Cao, and P. Lui, *Appl. Surf. Sci.*, **252**, 1634 (2005).
22. S. A. Umoren and E. E. Ebenso, *Mater. Chem. Phys.*, **106**, 387 (2007).
23. M. A. Quraishi, A. S. Mideen, M. A. W. Khan, and M. Ajmal. Indian, *J. Chem. Technol.*, **1**, 329 (1994).
24. S. Muralidharan, M. A. Quraish, and V. K. Iyer, *Corros. Sci.*, **37**, 1739 (1995).